Performance assessment of the ECMWF solar irradiation forecast in the Pampa Húmeda region of South America

Vívian Teixeira-Branco[1], Rodrigo Alonso-Suárez[2] and Mathieu David[3]

[1] Laboratorio Solar, ITR-Centro-Sur, Universidad Tecnológica, Durazno (Uruguay)

[2] Laboratorio de Energía Solar, Facultad de Ingeniería, Udelar, Montevideo (Uruguay)

[3] PIMENT Laboratory, University of La Réunion Saint-Denis (France)

Abstract

The increase in solar power generation has a direct impact on the management of the electrical grids, therefore knowing the resource availability for the next few hours and days becomes essential. In this article we present a performance evaluation of the solar predictions provided by the European Centre of Medium-Range Weather Forecasts (ECMWF) in different sites of the Pampa Humeda region, located in southeastern South America. It is found that the intraday hourly rRMSD ranges, on average, between 24.8% and 35.5% depending on the forecast horizon. For the daily integrated values, an increasing rRMSD trend between 16.6% and 21.3% is found for 1 to 3 days ahead, respectively. No significant geographical difference of the performance is observed between the sites. The uncertainty of this forecast model is lower than other numerical weather models previously evaluated in the region, which is consistent with international studies in other regions.

Keywords: solar forecast, NWP, GHI, ECMWF, Pampa Húmeda.

1. Introduction

The large deployment of grid-connected solar energy requires the ability to handle the fast fluctuations of the resource due to cloudiness variations. One way to accomplish this is to forecast the future resource, so an intelligent system reserves management can be done by grid operators. The uncertainty of the forecast directly translates to the decision-making process for optimal electricity dispatch and commercialization, thus impacting costs and revenues (Bridier et al. 2014; Lorenz et al., 2009). The development of accurate solar irradiation forecasting methods is then an important matter to further increase the solar energy shares into electricity grids. Consequently, evaluating the prediction data that is available for a region is considered to be of high value, as it provides an initial uncertainty reference (Yang et al., 2020). The determination of this uncertainty in most areas of studies consists of comparing the forecast outputs with ground-based measured data, which also have an error associated with the accuracy of the measurement (Blaga et al., 2019; Pérez et al., 2013).

There exist several methods to generate a solar forecast, namely, Numerical Weather Predictions (NWP), solar nowcasts based on geostationary satellite images or ground-based cameras, and machine learning strategies that attempt to learn from the previous data history or to combine different sources of forecast. NWPs, the subject of this work, address the forecast up to several days ahead with an hourly time resolution. This is achieved by using numerical atmospheric physical models that simulate the near future evolution of the atmosphere's state based on initial and boundary conditions, usually obtained by remote sensing strategies (atmospheric soundings, satellite retrievals, etc.). NWPs are known to outperform other sources of intra-day solar forecasts for the prediction above 5h ahead (Lorenz et al., 2007; Perez et al., 2010), in particular, hourly satellite nowcasts and machine learning techniques based solely on ground data. Furthermore, NWPs output are a required input variable for any form of day-ahead solar forecast that aims to have a competitive and reasonable performance. These models can be classified in two categories depending on their spatial scale, as different approximations hold true in the atmosphere's system equations: global models (i.e. GFS, ECMWF, etc.) and regional or mesoscale models (i.e. WRF, NAM, etc.), whose application is restricted to a regional area. The spatial and temporal resolution of such models are limited by the available computational capacity.

In this work we assess for the south-east of South America the solar predictions' uncertainty of the global model run by the European Center for Medium-Range Weather Forecast (ECMWF). The assessment is done for global solar irradiation at a horizontal plane (GHI) using controlled-quality ground measurements distributed in the region and without applying any post-processing technique to the forecasts. The evaluation includes the forecast up to 3 days ahead at hourly and daily-integrated time bases and incorporates an uncertainty analysis that discriminates the performance by the actual sky condition. A set of well-known statistical performance metrics are used for the assessment to facilitate comparison with other studies.

This article is organized as follows. Section 2 describes the GHI ground measurements being used, which are distributed throughout the Uruguayan territory and are representative of the wider Pampa Húmeda region of southeastern South America. Section 3 presents the main user-related characteristics of the ECMWF model, the persistence reference used here as benchmark and the performance metrics used for the evaluation. Section 4 presents the main results, which are divided into the hourly forecast evaluation and daily integrated forecast evaluation with and without sky conditions discrimination. Finally, Section 5 summarizes our conclusions.

2. Ground measurements

The measuring sites are presented in Tab. 1. These stations correspond to a field solar measurement network distributed in the Uruguayan territory and are located in rural or semi-rural environments. The sites are representative of the subtropical Pampa Húmeda region. This region is identified as Cfa in the updated Köppen-Geiger climate classification (Peel et al., 2007), being warm, temperate and humid with hot summers, and has an intermediate solar short-term variability (Alonso-Suárez et al., 2020).

The measuring stations are equipped with Kipp & Zonen Class A or B1 pyranometers according to the ISO 9060:2018 standard and receive monthly maintenance. These pyranometers are calibrated every two years, as recommended by the guidelines of the World Meteorological Organization, and following the ISO-9847:1992 standard by comparison with a Secondary Standard traceable to the World Radiometric Reference. The GHI data is recorded at a 1-minute interval, from which the 1-h averages were calculated. A basic quality control of the measurements was performed, based on the clearness index and the BRSN filters (McArthur, 2005). Under optimal operation conditions, the uncertainty assigned by the manuafacter to the equipments being used is of 2-3% on a daily scale. Given the current monthly routine maintenance and our regular inspections to the measuring sites, we assign a slightly higher effective uncertainty, between 4-5% (Laguarda et al., 2020). This value is also well below the uncertainty of the forecast to be evaluated.

Tab. 1: Details of the measurement stations used in the work.

Site	Code	Lat. (deg)	Lon. (deg)	Alt. (m)
Salto	LE	-31.28	-57.92	42
Artigas	AR	-30.40	-56.51	136
Tacuarembó	TA	-31.71	-55.83	140
Canelones	LB	-34.67	-56.34	32
Rocha	RC	-34.49	-56.17	24
Colonia	ZU	- 34.34	-57.69	81
Treinta y Tres	PP	-33.26	-54.49	58

3. NWP model and performance metrics

The ECMWF runs its global forecast model at 00 UTC each day, providing hourly forecasts of GHI up to several days ahead with a spatial resolution of 0.125° x 0.125° on latitude and longitude (approx. 14 x 14 km^2 in our region). We retrieved the first 72 hours of this forecast (3 days ahead) for each location of Tab. 1 and for the 2017-2018 period (two complete years).

As recommended (Yang et al., 2020) we use the clear-sky index (kc = Gh/Gh,csk) persistence as a reference to assess the performance of the forecasts. The GHI clear sky data (Gh,csk), required to compute the clear-sky index values, were downloaded from Copernicus Atmosphere Monitoring Service. This web service provides for free

clear sky irradiances estimates, derived from the McClear Model (Lefèvre et al., 2013). Any persistence reference involves the assumption that the atmospheric conditions are stationary in some sense. Here, since a days-ahead forecast is considered (issued during the previous night of the current day), the clear-sky index values of the previous day are persisted (calculated from the GHI measurements). For the hourly reference, the hourly clear sky daylight profile of the previous day is used, and for the daily-integrated evaluation, the daily clear sky index of the previous day is used, calculated as the ratio of the independent daily integration of Gh and Gh,csk.

To quantitatively evaluate the performance of the deterministic ECMWF forecast, we used common metrics (Yang et al., 2018): mean bias deviation (MBD), mean absolute deviation (MAD), root mean square deviation (RMSD) and forecasting skill (FS). The first metric measures the systematic bias of the forecast as compared to the measurements. The second and third metrics measure the dispersion of the deviations with different weighting norms, being the larger deviations more penalized by the RMSD than by the MAD. The last metric, FS, quantifies the gain of the method in terms of RMSD compared to the persistence benchmark. The metrics MBD, MAD and RMSD are defined in Eqs. (1), (2), (3), respectively:

$$MBD = \frac{1}{N}\sum_{I=1}^{N}(\hat{y}(i) - y(i)) \qquad (eq.1)$$

$$MAD = \frac{1}{N}\sum_{I=1}^{N}|\hat{y}(i) - y(i)| \qquad (eq.2)$$

$$RMSD = \sqrt{\frac{1}{N}(\hat{y}(i) - y(i))^2} \qquad (eq.3)$$

where $\hat{y}$ are the predicted values, y are the ground measured data and N is the number of observations. The relative values of these metrics, rMBD, rMAD and rRMSD, can be expressed as a percentage of the ground measurements average. In the case of the hourly evaluation, these relative metrics are found by using the GHI mean value for each hour of the day (an hourly daily profile of GHI). For the daily evaluation, the GHI daily average is simply used as normalization. Finally, the forecasting skill, FS, is defined as,

$$FS = 1 - \frac{RMSD_{forecast}}{RMSD_{persistence}} \qquad (eq.4)$$

being positive if the forecast outperforms the persistence and negative if not.

4. Results

4.1 Hourly forecast evaluation

The hourly performance evaluation of the ECMWF forecast and the persistence procedure up to 3 days ahead is summarized in Fig.1 (rMDB, rMAD and rRMSD) and Fig. 2 (FS). In these figures the performance metrics are plotted against the hourly forecast horizon (see the bottom *x* scale) or local time (see top *x* scale). The solid line represents the average performance over the sites of Tab. 1 and the area in transparency represents one standard deviation of the inter-sites performance, representing the spatial variability of the assessment. Tab. 2 presents the average performance metrics of the ECMWF forecast in relative terms for the three days. For the sake of clarity, the information contained in Fig. 1, Fig. 2 and Tab. 2 is only partial, for instance, the evaluation in each site is not represented and the metrics' absolute values are not given, among other detailed information that is not included. The complete set of performance metrics for each site, in absolute and relative terms, is available to the reader in the following download link: https://les.edu.uy/RDpub/ECMWF_local_evaluation.xlsx.

The overall analysis shows that the ECMWF forecast provides a better performance around solar noon with a slight downgrade with increasing forecast horizon, especially with increasing days. The ECMWF model performance is higher than the persistence procedure in all metrics, as expected. The ECMWF model has a low bias, with a tendency to overestimate before solar noon (first hours of the day) and a tendency to underestimate

after solar noon (late hours of the day). The trend towards underestimation increases with increasing days. The rMBD metric averaged between sites is contained between -3.7% to +3.7% for day 1, between -4.6% to 1.1% for day 2, and between -5.4% to +0.6% for day 3. The persistence procedure in all scenarios underestimates the resource, with a similar underestimation increase with increasing days. In the central hours the rRMSD of the ECMWF forecast varies between 24.9% (best, in day 1) and 37.5% (worst, in day 3). The persistence shows a similar increasing trend ranging from 36.5% (day 1) to 49.1% (day 3) around the solar midday of each day. The rRMSD variation in each day remains approximately constant for the ECMWF forecast, being of 8.8% for day 1 (24.9% to 33.7) of 8.5% for day 2 (from 27.3% to 35.7%) and of 8.2% for day 3 (from 29.3% to 37.5%). The rMAD presents similar behavior to the rRMSD, with the difference that the performance of the persistence (measured by this metric) tightens with the ECMWF model. The FS averaged between sites indicates that the performance of the ECMWF model is superior compared to the persistence procedure for all forecast horizons. Fig. 2 shows that the FS tends to decrease with increasing days and has a daily profile that peaks around the solar noon. The FS varies between 22.0% and 33.8% for day 1, between 23.3% and 33.0% for day 2 and between 21.4% and 29.6% for day 3.

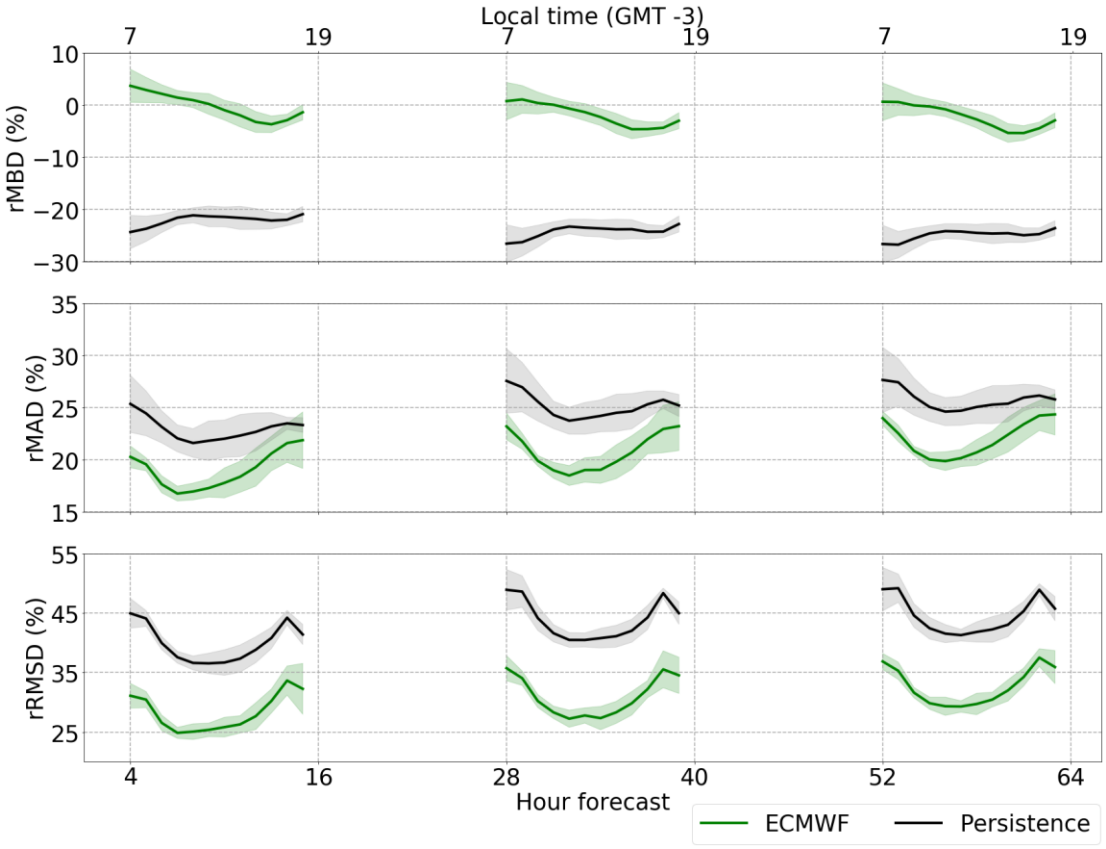

Fig. 1: Performance metrics of the ECMWF forecast at hourly resolution and up to 3 days ahead.

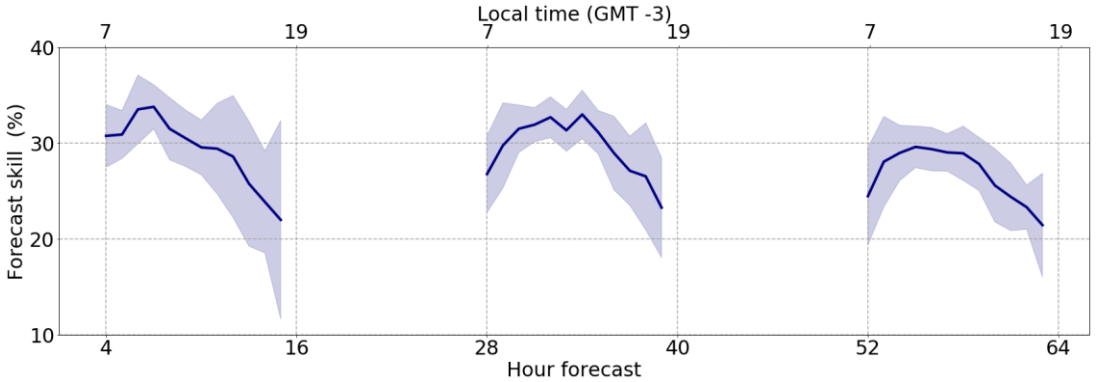

Fig. 2: Forecasting skill of the ECMWF forecast at hourly resolution and up to 3 days ahead.

Tab. 2: Hourly performance of the ECMWF model up to 3 days ahead.

Local time	Day 1			Day 2			Day3		
	rMBD (%)	rMAD (%)	rRMSD (%)	rMBD (%)	rMAD (%)	rRMSD (%)	rMBD (%)	rMAD (%)	rRMSD (%)
7	+3.7	20.3	31.1	+0.8	23.2	35.7	+0.6	24.0	36.9
8	+2.9	19.5	30.5	+1.1	21.8	34.0	+0.6	22.5	35.3
9	+2.2	17.6	26.5	+0.4	19.9	30.2	-0.1	20.8	31.6
10	+1.4	16.7	24.9	+0.1	19.0	28.3	-0.3	20.0	29.8
11	+1.0	16.9	25.1	-0.7	18.5	27.3	-0.8	19.8	29.3
12	+0.2	17.3	25.4	-1.3	19.0	27.8	-1.8	20.1	29.3
13	-1.0	17.8	25.8	-2.3	19.0	27.3	-2.7	20.7	29.7
14	-2.0	18.3	26.3	-3.5	19.8	28.3	-4.0	21.4	30.5
15	-3.2	19.3	27.7	-4.6	20.7	29.8	-5.3	22.4	32.0
16	-3.7	20.6	30.2	-4.6	22.0	32.2	-5.4	23.4	34.2
17	-2.9	21.6	33.7	-4.4	22.9	35.5	-4.4	24.2	37.5
18	-1.4	21.9	32.3	-3.0	23.2	34.5	-2.9	24.3	35.9

Previous evaluations of NWPs in the region are given in Porrini et al. (2017) and Teixeira-Branco et al. (2018). These works used the WRF (Weather Research and Forecasting) mesoscale model with its initial and boundary conditions taken from the GFS (Global Forecast System) global model forecast and different parameterizations (microphysics, boundary layer, solar radiation, among others) to predict GHI in the same region of this study. Porrini et al. (2017) provides an hourly evaluation of the GFS driven WRF forecast, and found site averages of rMBD around +12-14% and rRMSD around 40-44% for day 1 close to the solar midday. The performance found here for the ECMWF forecast is significantly better.

4.2 Daily accumulated forecast evaluation

On a daily scale, the results are presented for the first forecast day by integrating the first 24h (1 day ahead), the second forecast day by integrating the hourly horizons from 25h to 48h (2 days ahead) and the third forecast day by integrating from 49h to 72h (3 days ahead). Tab. 3 shows the ECMWF model performance metrics on a daily scale and discriminating by each site, in absolute and relative terms. For compatibility with previous studies, the absolute values are presented in MJ/m^2. If desired, it is possible to convert them to kWh/m^2, by dividing them between 3.6. Tab. 4 shows the same information but averaged over all sites.

Tab. 3: Performance of the ECMWF model for daily-integrated predictions up to 3 days ahead and discriminated by each site.

	N	Mean GHI (MJ/m^2)	MBD (MJ/m^2)	MAD (MJ/m^2)	RMSD (MJ/m^2)	rMBD (%)	rMAD (%)	rRMSD (%)	FS (%)
LE									
day 1	718		-0.3	2.1	2.9	-1.8	12.1	16.7	57.4
day 2	717	17.5	-0.5	2.4	3.4	-3.2	14.0	19.5	58.0
day 3	716		-0.7	2.7	3.8	-4.1	15.5	22.0	58.5

AR									
day 1	702		0.0	2.9	2.9	-0.1	11.9	16.9	56.8
day 2	701	17.5	-0.3	2.4	3.5	-2.0	13.7	19.8	55.7
day 3	700		-0.4	2.6	3.8	-2.5	15.1	21.8	51.9
TA									
day 1	724		-0.1	2.0	2.9	-0.7	12.2	16.9	57.7
day 2	723	17.0	-0.5	2.4	3.4	-2.7	13.9	20.2	57.2
day 3	722		-0.8	2.6	3.8	-4.5	15.6	22.5	54.5
LB									
day 1	724		0.0	1.9	2.6	-0.4	11.3	15.5	61.5
day 2	723	16.8	-0.2	2.2	3.0	-1.2	13.1	18.2	59.8
day 3	722		-0.1	2.4	3.4	-0.8	14.6	20.4	56.3
RC									
day 1	724		0.0	2.0	2.8	-0.1	12.6	17.2	58.4
day 2	723	16.2	-0.3	2.4	3.3	-2.1	14.8	20.5	56.7
day 3	722		-0.2	2.5	3.5	-1.6	15.6	22.0	54.8
ZU									
day 1	724		+0.4	1.8	2.7	+2.5	10.8	16.2	61.5
day 2	723	16.8	+0.4	2.1	3.0	+2.7	12.5	18.2	60.9
day 3	722		+0.4	2.3	3.3	+2.4	13.6	19.8	59.3
PP									
day 1	715		-0.3	2.0	2.8	-1.7	12.1	16.8	54.0
day 2	714	16.8	-0.6	2.1	3.1	-3.7	13.0	18.5	57.6
day 3	713		-0.7	2.5	3.5	-4.1	14.8	20.8	54.8

Tab. 4: Performance of the ECMWF model averaged over all sites for daily-integrated predictions up to 3 days ahead.

	Mean GHI (MJ/m^2)	**MBD (MJ/m^2)**	**MAD (MJ/m^2)**	**RMSD (MJ/m^2)**	**rMBD (%)**	**rMAD (%)**	**rRMSD (%)**	**FS (%)**
day 1		≈ 0.0	2.1	2.8	-0.3	11.8	16.6	58.2
day 2	16.9	-0.3	2.3	3.2	-1.4	13.6	19.3	58.0
day 3		-0.3	2.5	3.6	-2.2	14.9	21.3	55.7

The performance of the ECMWF forecast is better at the daily-integrated time scale than at the hourly time resolution, as expected. Not only the MBD, MAD and RMSD are significantly lower, but also the FS is higher. The daily bias of the predictions tends towards underestimation and is low, ranging between +2.7% and -4.5% across sites and forecast horizons, and with a site average between -0.3% (day 1) and -2.2% (day 3), confirming the increasing trend towards underestimation with the forecast horizons. The ECMWF forecast's RMSD has increasing values with increasing days. The rRMSD varies across sites between 15.5% and 17.2% for day 1,

between 18.2% and 20.2% for day 2 and between 19.8% and 22.5% for day 3. In average terms, the rRMSD of the ECMWF forecast increases from 16.6% at day 1 to 21.3% at day 3. The persistence has higher rRMSD values (ranging from 39.7% to 47.8% for 1 to 3 days ahead, respectively), arising to the high FS values obtained for ECMWF daily forecast, as shown in Tab. 4. Fig. 3 shows the rRMSD trend for the daily integrated values, discriminated by each site (Fig. 3a) and site-averaged (Fig. 3b, which also includes the persistence rRMSD values). There is a slight variability of performance across the sites in the region, as shown by the little difference in the bars of Fig. 3a. The MAD metric averaged between sites presents increasing values from 2.1 MJ/m^2 for day 1 to 2.5 MJ/m^2 for day 3, which in percentage correspond respectively to 11.8% and 14.9%.

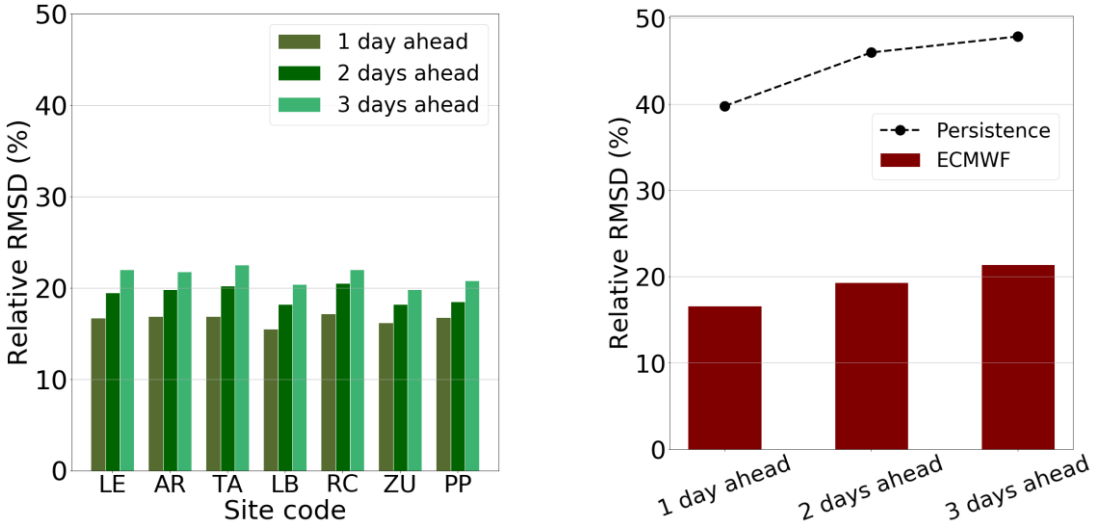

(a) ECMWF model accuracy by site **(b) average performance of the sites**

Fig.3: Performance model daily forecast.

Other studies in other parts of the world, i.e.. Lauret et al. (2016), Remund et al. (2008), Perez et al. (2013) and Lorenz et al. (2009) reported performance evaluations of the daily-integrated ECMWF forecast, with rMAD values ranging from 14% to 32% and rRMSD values ranging from 22% and 45% for 1 to 3 days ahead, respectively. Comparing our results with these studies is not straightforward, as each evaluation has its own particularities. Some varying conditions are the spatial resolution of the model, the climate characteristics at each site, specially its short-term solar irradiance variability caused by unstable sky conditions that are difficult to predict, and the use of temporal interpolation techniques to convert a 3h forecast into a 1h forecast. Likewise, our results are similar and slightly better to those reported in the Perez et al. (2013) for the southern region of Spain, at altitude and latitude similars to that of the Pampa Humeda region, with an rRMSD ranging from 22% to 29% for 1 to 3 days ahead.

Daily-integrated forecasts evaluations of NWPs in our region are presented in Porrini et al. (2017) and Teixeira-Branco et al. (2018), using the GFS-driven WRF up to 3 days ahead as mentioned before. According to Porrini et al., the WRF+GFS strategy showed an average rRMSD ranging from 27% to 39% for 1 to 3 days ahead, respectively. On the other hand, Teixeira-Branco et al. (2018) reported an irradiation overestimation of 22% and rRMSD values ranging from 43% to 51% for the same time horizons and using the same initial and boundary conditions. These differences are explained by the different parameterizations used for the WRF in both works. The ECMWF forecast provides better performance than the previously tested joint use of GFS and WRF, which up to date are the only models evaluated for the region with extended data sets.

4.3 Evaluation of the performance's dependence on sky conditions

In this section we present the ECMWF model's performance for the daily-integrated GHI forecast as a function of daily average sky conditions. This discrimination is achieved by using the daily clearness index (K_T) which is the result of dividing the GHI ground measurements by irradiation incident on a horizontal surface at the top of the atmosphere, as a proxy. The three considered daily conditions are: clear sky (K_T above 0.65), partly cloudy (K_T between 0.65 and 0.35) and cloudy or overcast (K_T below 0.35). These ranges have been determined from visual inspection of the clarity index histograms and are similar to those reported by Fanego et al. (2012). During

the evaluated period the clear sky days represent about 41% of the samples, the partly cloudy days about 38% of the samples and the overcast days around 21% of the samples. The results are presented in Tab. 5 and Fig. 4, averaged across all sites.

As it can be seen from Tab. 5 and Fig. 4, both metrics (MBD and RMSD) increase with the forecast horizon (days ahead) for each sky condition, as expected. For cloudy conditions the forecast model shows important overestimation figures, with rMBD between +38.5% to +41.7%. It is clear that the models underrepresents the occurrence of cloudiness and, in particular, the overcast sky condition is importantly misrepresented. As a consequence, the rRMSD obtained is also very high for this sky condition, being between 68.3-78.4%. It shall be noted that although these relative metrics are high, the absolute indicators are not so notable, being approximately around 2 MJ/m^2 for MBD and between 3.7-4.2 MJ/m^2 for RMSD. The model's forecast presents its lower biases under partly cloudy sky conditions. For day 1 it is almost unbiased (MBD $\simeq$ 0), and for day 2 and 3 it presents a slight underestimation, around -2%. The rRMSD are intermediate for this sky condition, ranging from 16.1% to 23.6% for day 1 and 3, respectively. The clear sky irradiation is underestimated (rMDB between -5.4% and -7.3%), for instance, the bias is higher than under partly cloudy conditions. By inspecting the data scatterplots for this clear sky evaluation, we have observed that this underestimation is caused by some incorrectly forecasted clouds, i.e. it is not caused by an underrepresentation of the clear sky irradiation. Although the clear sky MBD is not the lowest in these three sets, the RMSD shows its best figures (between 8.5% and 12.4%). This is of course associated with the lower variability of the clear sky data in comparison to cloudy conditions. Fig. 4 illustrates the previous comments based on the absolute metrics.

Tab. 5: Daily-integrated performance evaluation discriminated by sky condition (using K_T as proxy).

Forecast horizon	Sky conditions	Mean GHI (MJ/m^2)	MBD (MJ/m^2)	RMSD (MJ/m^2)	rMBD (%)	rRMSD (%)
day 1						
	Clear sky	23.6	-1.2	2.0	-5.4	8.5
	Partly cloudy	16.1	$\simeq$0.0	2.9	+0.2	16.1
	Cloudy	5.5	+2.0	3.7	+38.5	68.3
day 2						
	Clear sky	23.6	-1.5	2.6	-6.4	10.9
	Partly cloudy	16.1	-0.3	3.4	-1.8	21.4
	Cloudy	5.5	+2.0	3.9	+37.6	72.2
day 3						
	Clear sky	23.6	-1.7	2.9	-7.3	12.4
	Partly cloudy	16.1	-0.4	3.8	-2.4	23.6
	Cloudy	5.5	+2.2	4.2	+41.7	78.4

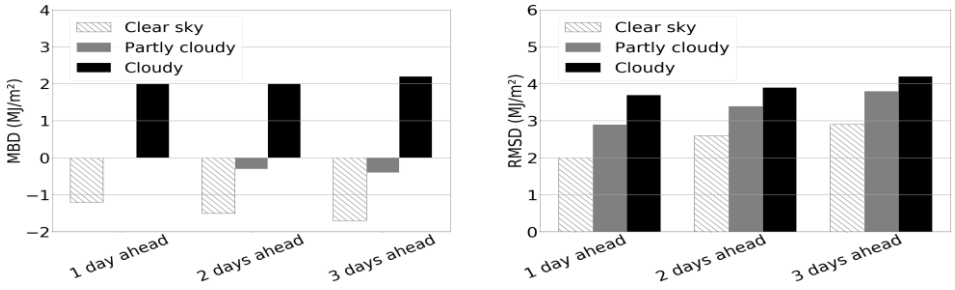

Fig.4: Daily-integrated performance evaluation discriminated by sky condition.

In sum, this work have validated for the Pampa Húmeda region some previous knowledge about the general performance of the ECMWF model for solar irradiation forecast: (i) the model's performance is one of the best of its kind, being to date the best performing NWP in our region (in comparison to the ones that have been previously evaluated with extended controlled-quality data sets), (ii) the model presents some difficulties to forecast the occurrence of clouds, specially for very low clearness index days. The GHI forecast of the ECMWF model varies its bias behavior with the presence or absence of cloudiness, from underestimation under clear sky conditions to overestimation under overcast situations. In spite of these deficiencies, the gains with respect to the previous application of other NWP models in the region are quite significant.

5. Conclusions

A performance evaluation of the GHI predictions provided by the global ECMWF model is presented for the Pampa Húmeda region, using two years of controlled-quality measured data registered at seven sites distributed in the Uruguayan territory. The model's performance assessment is done on an hourly and daily-integrated time scales, and for the second time basis, it also includes a discrimination by different sky conditions based on the daily clearness index. To quantify the forecast uncertainty we employ the most commonly used statistical indicators in the field, namely, the MBD, MAD, RMSD and FS. The evaluation is aimed to provide useful operational information on the ECMWF model's overall performance in the region, characterizing its typical uncertainty and detecting predictions' drawbacks.

By assessing the GHI forecast at individual sites, we found no significant spatial variability on the model's performance, indicating that the model's uncertainty does not have a marked geographical dependence. The predictions clearly outperform the persistence benchmark for all metrics and in both time scales. The hourly performance evaluation indicates that the ECMWF solar forecast has a better performance in the central hours of the day and increasing negative biases towards the end of the day and with increasing forecast horizon. For daily integrated values the predictions have a low underestimating bias (rMBD between zero and approximately -2%) and overall rRMSD between ≃17-21%, increasing in this range with the forecast horizon (days ahead). A dependence of the model's performance with the average cloudiness of each day is found. An important overestimation bias is observed for cloudy (overcast) conditions. This overestimation can reach +38-42% of rMBD and affects the rest of the performance metrics under this condition. The bias figure is not so high in absolute terms, being of approximately 2 MJ/m^2, but anyway is the highest of the three sky conditions analyzed here. On the other hand, the models underestimates the solar irradiation under clear-sky conditions, due to some incorrectly forecasted clouds.

The performance found for the ECMWF solar forecast is the best observed to date for a NWP in the region, which is consistent with previously reported studies in other regions. Furthermore, this is the first assessment of the solar predictions of this model in the Pampa Húmeda region, which allows us to compare it with other forecasting models, previously evaluated in the region. This work can be complemented with the diagnosis of other global models for solar prediction in the region, in order to identify their weaknesses and strengths, and thus define strategies to reduce the solar prediction uncertainty, which is part of our current work.

References

Alonso-Suárez, R., David, M., Texeira-Branco, V., Lauret, P., 2020. Intra-day solar probabilistic forecasts including local short-term variability and satellite information. Renewable Energy 158:554-573. https://doi.org/10.1016/j.renene.2020.05.046.

Bridier, L.; David, M.; Lauret, P., 2014. Optimal design of a storage system coupled with intermittent renewables. Renew. Energy 67, 2–9. https://doi.org/10.1016/j.renene.2013.11.048.

Blaga, R., Sabadus, A., Stefu, N., Dughir, C., Paulescu, M., Badescu, V., 2019. A current perspective on the accuracy of incoming solar energy forecasting. Prog. Energy Combust. Sci. 70, 119–144. https://doi.org/10.1016/j.pecs.2018.10.003

McArthur, L., 2005. Baseline Surface Radiation Network (BSRN) Operations Manual. Td-no. 1274, wrcp/wmo, World Meteorological Organization (WMO).

Lara-Fanego, V., Ruiz-Arias, J.A., Pozo-Vázquez, D., Santos-Alamillos, F.J., Tovar-Pescador, J., 2012. Evaluation of the WRF model solar irradiance forecasts in Andalusia (southern Spain). Solar Energy 86:2200-2217. https://doi.org/10.1016/j.solener.2011.02.014.

Lauret, P.; Lorenz, E.; David, M., 2016. Solar Forecasting in a Challenging Insular Context. Atmosphere 7, 18.8. ECMWF. https://doi.org/10.3390/atmos7020018

Lefèvre, M., Oumbe, A., Blanc, P., Espinar, B., Qu, Z., Wald, L., Homscheidt, M. S., and Arola, A., 2013. McClear: a new model estimating downwelling solar radiation at ground level in clear-sky conditions. Atmospheric Measurement Techniques, European Geosciences Union, 6:2403–2418.

Laguarda, A., Giacosa, G., Alonso-Suárez, R., Abal, G., 2020. Performance of the site-adapted CAMS database and locally adjusted cloud index models for estimating global solar horizontal irradiation over the Pampa Húmeda. Solar Energy, 199:295-307. https://doi.org/10.1016/j.solener.2020.02.005.

Lorenz, E., Heinemann, D., Wickramarathne, H., Beyer, H.G., Bofinger, S., 2007. Forecast of ensemble power production by grid-connected PV systems. In: Proc. 20th European PV Conference, Milano, Italy.

Lorenz E, Hurka J, Heinemann D, Beyer HG., 2009. Irradiance forecasting for the power prediction of grid-connected photovoltaic systems. IEEE Journal of Selected Topics in Applied Earth Observations and Remote Sensing 2:2–10. https://doi.org/10.1109/JSTARS.2009.2020300

Peel, M. C., Finlayson, B. L., & Mcmahon, T. A., 2007. Updated world map of the köppen-geiger climate classification. Hydrology and Earth System Sciences Discussions, 11, 1633–1644. https://doi.org/10.5194/hess-11-1633-2007

Perez, R., Kivalov, S., Schlemmer, J., Hemker Jr., K., Renne, D., Hoff, T., 2010. Validation of short and medium term operational solar radiation forecasts in the US. Solar Energy 84 (12), 2161–2172. https://doi.org/10.1016/j.solener.2010.08.014.

Perez, R., et al., 2013. Comparison of numerical weather prediction solar irradiance forecasts in the US, Canada and Europe. Solar Energy, 94:305–326. https://doi.org/10.1016/j.solener.2013.05.005.

Porrini, C., Boezio, G., 2017. Evaluación de modelos numéricos para pronósticos de radiación solar para plazos de hasta 120 horas en territorio uruguayo. Tesis de Grado en Licenciatura en Ciencias de la Atmósfera, Facultad de Ingeniería y Facultad de Ciencias, UdelaR.

Remund, J., Perez, R., Lorenz, E., 2008. Comparison of solar radiation forecasts for the USA. In: 2008 European PV Conference, Valencia, Spain.

Teixeira-Branco, V., Alonso-Suárez, R., de Almeida, E., Porrini, C., Gutiérrez, A., Cazes, G, 2018. Evaluación del pronóstico de irradiación solar diaria en Uruguay utilizando el modelo WRF. Anais do VII Congresso Brasileiro de Energia Solar (CBENS), ISBN: 978-85-62179-02-0, Gramado, Brasil.

Yang, D., Kleissl, J., Gueymard, C.A., Pedro, H.T.C., Coimbra, C.F.M., 2018. History and trends in solar irradiance and PV power forecasting: A preliminary assessment and review using text mining. Solar Energy 168, 60–101. Advances in Solar Resource Assessment and Forecasting. https://doi.org/10.1016/j.solener.2017.11.023.

Yang, D., et al., 2020. Verification of deterministic solar forecasts. Solar Energy 210:20-37. https://doi.org/10.1016/j.solener.2020.04.019.

.